

530-18
N88-15631 116732
238

1987

NASA/ASEE SUMMER FACULTY RESEARCH FELLOWSHIP PROGRAM

MARSHALL SPACE FLIGHT CENTER
THE UNIVERSITY OF ALABAMA IN HUNTSVILLE

TETHER ELEVATOR CRAWLER SYSTEMS (TECS)

Prepared by:	Frank R. Swenson
Academic Rank:	Professor
University and Department:	Tri-State University Mechanical and Aerospace Engineering
NASA/MSFC:	
Directorate:	Program Development
Office:	Advanced Systems
Group:	Orbital Support Systems
NASA Colleagues:	James K. Harrison Charles C. Rupp
Date:	August 24, 1987
Contract No:	The University of Alabama in Huntsville NGT-01-008-021

ABSTRACT

One of the needs of experimenters on Space Station is the access to steady and controlled-variation microgravity environments. A method of providing these environments is to place the experiment on a tether attached to the Space Station. This provides a high degree of isolation from structural oscillations and vibrations. Crawlers can move these experiments along the tethers to preferred locations, much like an elevator. This report describes the motion control laws that have been developed for these crawlers and the testing of laboratory models of these tether elevator crawlers.

ACKNOWLEDGEMENTS

The author wishes to acknowledge the NASA/ASEE Summer Faculty Fellowship Program, along with Dr. Gerald Karr, the UAH University Program Co-Director, and Ms. Ernestine Cothran, the NASA/MSFC Co-Director.

To NASA counterparts Mr. James K. Harrison and Mr. Charles C. Rupp of the Orbital Support Systems Group, Advanced Systems Office of the Program Development Directorate, a very special thanks is offered for their help with the analytical, assembly, design and organizational activities.

A further thanks is due to Mr. James P. McGee and Mr. James B. Herring of the Dynamics Test Branch, Structural Test Division, of the Test Laboratory for their assistance with the experimental activities.

LIST OF FIGURES

<u>Figure Number</u>	<u>Title</u>	<u>Page:XXXI-</u>
1.	Crawler Motion Control Laws	6
2.	Mirror Image Motion Control Law (MIMCL): Characteristic Curves	7
3.	Three Successive Phases of the Mirror Image Motion Control Law	8
4.	Time to Travel Total Distance: Mirror Image Motion Control Law	9
5.	Comparison of Motion Control Laws: Distance Travelled versus Time	10
6.	Comparison of Motion Control Laws: Velocity versus Time	11
7.	Comparison of Motion Control Laws: Acceleration versus Time	12
8.	Tether Crawler Engagement Mechanism and Drive Train	13
9.	Drive Control System	14
10.	6-Ft Air Table	15
11.	32-ft Air Table	16
12.	TECS Schedule: 1987-1990	17
13.	Tether Elevator Crawler System (TECS): Shuttle Flight Demonstration	18

1. Introduction

Tethers attached to orbiting spacecraft can be used to provide parking locations and paths for microgravity environment experiments if a crawler system moves the experiment along the tether. Two tether configurations are possible - one, a clothesline configuration, in which both ends of the tether are rigidly fixed to the spacecraft structure; and the second, a free end mass or pendant configuration, in which one end is fixed to the spacecraft and the other to an end mass which by gravity-gradient forces pulls the tether taut either outward from the center of the orbit or inward toward the center of the orbit.

These two tether configurations have different environment ranges and provide conditions for different types of microgravity experiments. These differences can be stated as:

Fixed Ends (Clothesline)

- Steady G-Level Experiments
- 10^{-5} to 10^{-2} G

Free-End Mass (Pendant)

- Variable-G Experiments
- Microgravity, 10^{-6} to 10^{-5} G.

Crawler motions in space along a tether are a combination of the responses to the instructions of a motion control law, to the vibrations transmitted from the spacecraft, and to the dynamics of motion of the entire orbiting tether/crawler system. The response to each of these is of interest in this study.

2. Mirror Image Motion Control Law (MIMCL)

A number of control laws (Fig 1) for the motion of a crawler along a tether have been developed starting with Rupp (1) in 1975. A major step to provide more flexibility by independently controlling the maximum velocity and accelerations during the motion was made in the hyperbolic tangent motion control law developed by Lorenzini (2) in 1986. This new control law was one continuous function throughout the motion and had a smooth acceleration from rest to a peak velocity followed immediately by a smooth deceleration which approached zero velocity exponentially so that a cutoff distance had to be introduced to terminate the motion at a small but finite velocity and a selected small proximity to the total distance. In this motion control law the peak deceleration is smaller than the peak acceleration and the time interval for deceleration is much longer than the time interval for acceleration. However, the slow initial accelerations and final decelerations made this very attractive as a motion control law, especially when operating a crawler close to the spacecraft on a pendant (free end mass) configuration tether.

Later in the same year, Swenson (3) added a constant-velocity middle phase to the hyperbolic tangent control law at the maximum velocity point where the acceleration was zero. This retained the advantages of the hyperbolic tangent motion control law but also allowed the same distance to be covered in the same time interval but with a lower value of peak acceleration. However, even this modification did not eliminate either the time-inefficient, long exponential tail of the hyperbolic tangent motion control law or the necessity of stopping the motion when the velocity was small but still finite and at a cutoff distance from the expected end of the motion.

In 1987 Rupp and Swenson (4) changed the tail end of the modified hyperbolic tangent motion control law so that the deceleration tail was the mirror image of the acceleration beginning of the motion. This resulted in symmetrical motion curves (Fig 2) in distance, velocity and acceleration. The motion then occurs in three successive phases (Fig 3) in which the acceleration and deceleration phases are mirror images of each other and the peak acceleration and the peak deceleration have the same value.

The equation of motion during the beginning acceleration phase is:

$$L(t) = \Delta L_c' [\tanh(\alpha t)]^\gamma, 0 \leq t \leq t_A \quad (1)$$

where, the time at the end of the acceleration phase is:

$$t_A = \frac{1}{\alpha} \sinh^{-1} \left[\sqrt{\frac{\gamma-1}{2}} \right] \quad (2)$$

and, the maximum velocity is:

$$L'_{c,m} = \Delta L_c' \alpha \left[\frac{2\gamma}{\gamma+1} \right] \left[\frac{\gamma-1}{\gamma+1} \right]^{\frac{\gamma-1}{2}} \quad (3)$$

The mirror image motion control law provides the system designer and the tether elevator crawler system motion programmer with considerable flexibility, part of which can be shown with these equations for this first phase. The parameters in the equations for the hyperbolic tangent acceleration and deceleration phases of the motion are the distance parameter, $\Delta L_c'$, the time parameter, α ; and the shape parameter, γ . Two advantages that go back to using the power function of the hyperbolic tangent function as a motion control law are that the time to reach maximum velocity (zero acceleration point) is independent of the selected distance interval and that the maximum velocity function can be divided by the distance interval to give another function which depends only on the values of the time parameter and the shape parameter. With three independent parameters in the equations, independent selections may be made of the distance, the maximum velocity and the time to reach maximum velocity.

The addition of the constant-velocity phase increases the flexibility to the motion control law user by adding a section of travel at maximum velocity along the tether which has a distance parameter, $\Delta L_c''$, which is independent of the other parameters. The transition into this phase is also smooth as it is made at the point of zero acceleration. The equation for the total distance travelled through the acceleration phase and to the end of the constant-velocity phase is:

$$L(t) = \Delta L_c' [\tanh(\alpha t_A)] + \dot{L}_{c,m} (t - t_A), \quad t_A \leq t \leq t_B \quad (4)$$

where, the time to the end of the constant-velocity phase is:

$$t_B = t_A + \frac{\Delta L_c''}{\dot{L}_{c,m}} \quad (5)$$

Another aspect of this flexibility is that the time interval for this phase, $t_B - t_A$, is a function only of the distance to be travelled at constant velocity and the value of the maximum velocity.

Being a mirror image, the deceleration phase is already determined by the parameters selection for the acceleration phase. The equation for distance in this phase is:

$$L(t) = \Delta L_T - \Delta L_c' \{ \tanh[\alpha(t_T - t)] \}, \quad t_B \leq t \leq t_T \quad (6)$$

where, the total distance travelled during the three phases of the motion is:

$$\Delta L_T = \Delta L_c' + \Delta L_c'' \quad (7)$$

and the total time to travel this total distance is:

$$t_T = t_A + (t_B - t_A) + t_A = t_A + t_B \quad (8)$$

A summary of the features of the mirror image motion control law is:

- smooth accelerations and decelerations
- smooth transitions
- three independent acceleration and deceleration phases parameters
- one independent constant-velocity phase parameter.

The mirror image motion control law (MIMCL) is very time efficient (Fig 4). When comparison is made to the modified hyperbolic tangent motion control law (MHTMCL), the shortening in travel time can be seen in graphs for distance (Fig 5), velocity (Fig 6), and acceleration (Fig 7). For the same total distance traveled (4km in Figs 5 and 6, 384-in in Fig 7) and the same values of equation time and shape parameters, the motions using two forms of the mirror image motion control law (MIMCL) both end much quicker than with the modified hyperbolic tangent motion control law (MHTMCL).

Additional conclusions can be reached from the curves. For the same control law equation parameters, the change to a mirror image always results in a shorter time for deceleration. It also results in the shorter distance travelled during deceleration becoming the same distance as the acceleration distance. The result is that the sum of the nominal distances for acceleration, deceleration and constant-velocity is larger than the distance actually travelled, and an adjustment must be made in either the nominal distance to calculate the acceleration and deceleration phases or in the distance actually travelled during the constant-velocity phase.

Therefore, there are two possible forms of the mirror image motion control law that correspond to the same modified hyperbolic tangent motion control law. If the fraction, Y , of the total distance that is at constant-velocity is the same in the MIMCL and the MHTMCL, then the time to complete the motion is shortest. However, the peak acceleration and deceleration are increased to higher values. If the fraction, X , of total distance for acceleration and deceleration is kept the same in the MIMCL as in the MHTMCL, then an intermediate value of travel time results. The peak values of acceleration are the same and the peak value of deceleration in the MIMCL is equal to the peak value of acceleration.

The mirror image motion control law has features which make it the best to date in this series of the tether elevator motion control laws and can be used as a standard for comparison of motion control laws.

Lorenzini (5) has recently developed a retarded exponential (RE) motion control law which is especially useful for short-distance maneuvers. It is another step forward in this succession of motion control laws.

3. Crawler System Development and Testing

The tether crawler system that has been developed has the engagement mechanism and drive train similar to those shown in Fig 8. The tether is gripped between a toothed drive wheel and a toothed belt. The drive wheel moves both the tether and the belt and the entire system crawls up or down along the tether. If there is no slip between the drive and the tether, the position change of the crawler along the tether can be found from measurement of the rotation of the drive wheel.

A control system (Fig 9) has been developed to control the drive system to follow inputs from a motion control law that is a real-time model in a microprocessor. The desired location and velocity from the model are compared with the measured location and/or velocity to give an error signal that drives the motor. Two types of motors - stepping motors and DC motors - are being used in three different laboratory crawler systems.

Two flat-surface tables are being used for testing the crawler drive and control systems. The first, a 6-foot long glass

surface (Fig 10) is used for crawler and instrumentation system development. The second, a 32-foot long plastic surface (Fig 11), is being built for the testing of crawler/tether system dynamics. Both tables have the tether suspended horizontally over the length of the flat surface and have strain gages mounted on the end supports for the measurement of tether tension forces in the segments in front and in back of the moving crawler. For two-dimensional testing, the crawler rides on an air film that is generated by an air bearing. This thin film provides very-low frictional resistance to longitudinal (along the tether) and lateral movements of the crawler.

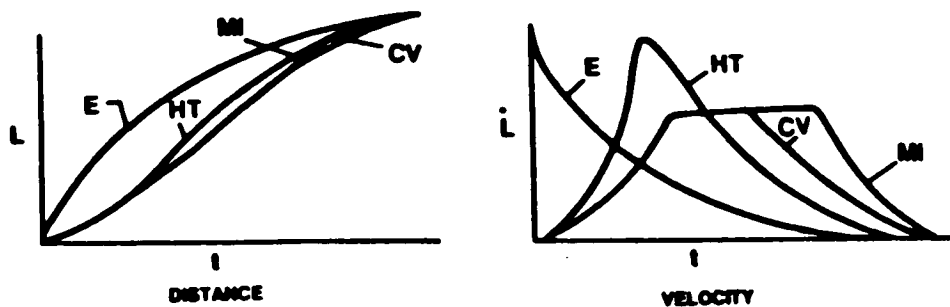
The end conditions of the tether may be changed from being rigidly attached to the end support to give a fixed-end condition to going through a hole in the end support to give a free-end condition. Strain gages attached to the sides of the end support sense the changes in tether tension and accelerometers sense the movements of the crawler. An infra-red communications link is being developed to replace the present electrical umbilical which carries instructions and information to and from the crawler system.

In summary, a list of the components that are part of the crawler system is

- tether engagement mechanism
- drive train
- drive control system
- acceleration measurement
- communications link
- on-board microprocessor.

The testing equipment is represented in the Figs 10 and 11 by the trajectory grids underneath the clear, flat surfaces; the tension sensors on the end supports; the preprocessor which sends motion law parameter values to the microprocessor on-board the crawler; the tether tension recorder and the time-base counter. Not shown are the magnetic tape recorders for data storage, the on-board flasher unit, and the videocamera and still camera for recording the crawler trajectories.

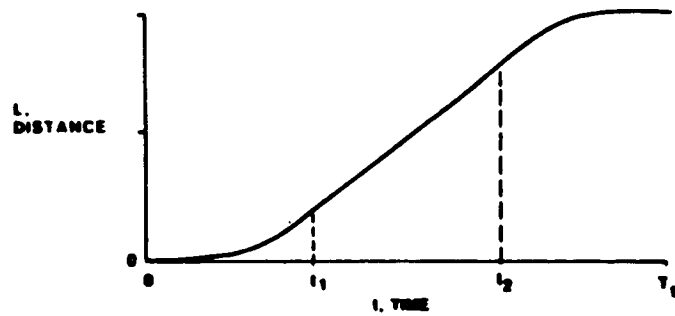
All of these development and testing activities are part of the schedule (Fig 12) for the tether elevator crawler systems. The demonstration flights on balloon, KC-135 and rocket vehicles are all paths to the demonstration of tether elevator crawler system (TECS) capabilities in space on board the Shuttle (Fig 13). This demonstration on a clothesline-configuration tether will culminate the initial development and testing of the TECS. Then it will be ready for application on board the Space Station.



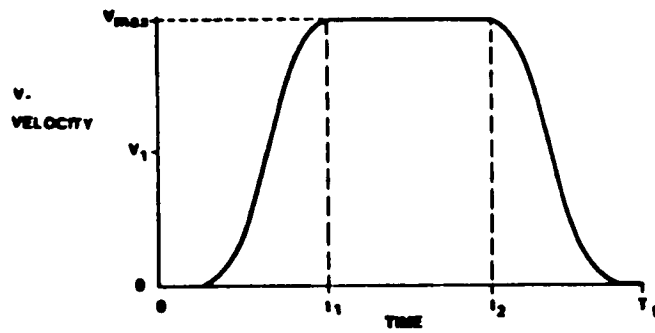
- EXPONENTIAL (RUPP 1975)
- HYPERBOLIC TANGENT (LORENZINI 1986)
- CONSTANT-VELOCITY ADDITION (SWENSON 1986)
- MIRROR IMAGE (RUPP/SWENSON 1987)

TETHER CRAWLER MOTION CONTROL LAWS

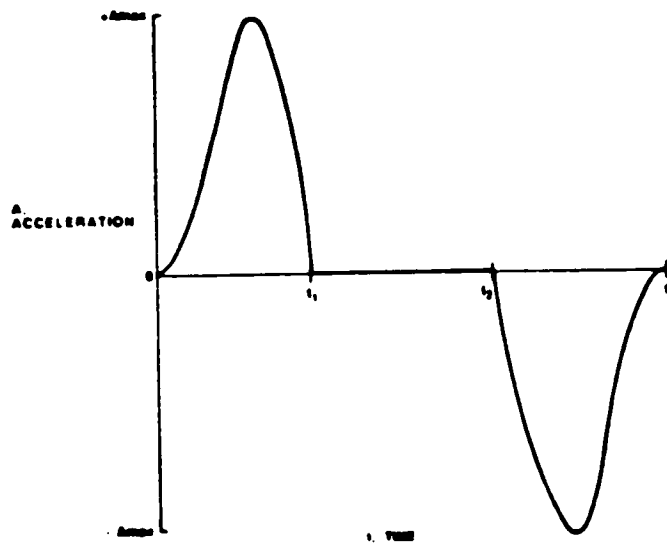
FIG 1



DISTANCE TRAVELED VERSUS TIME -

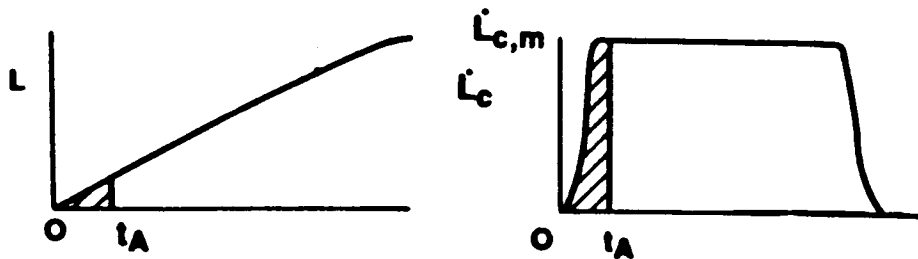


VELOCITY VERSUS TIME

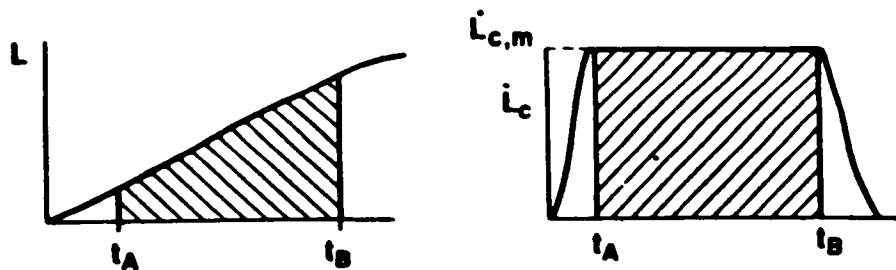


ACCELERATION VERSUS TIME

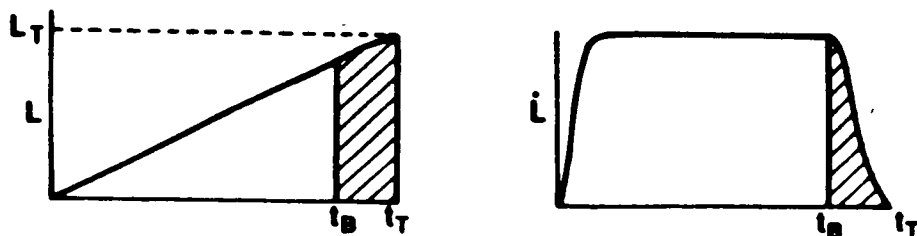
FIG 2 MIRROR IMAGE MOTION CONTROL LAW:
CHARACTERISTIC CURVES



ACCELERATION PHASE



CONSTANT-VELOCITY PHASE

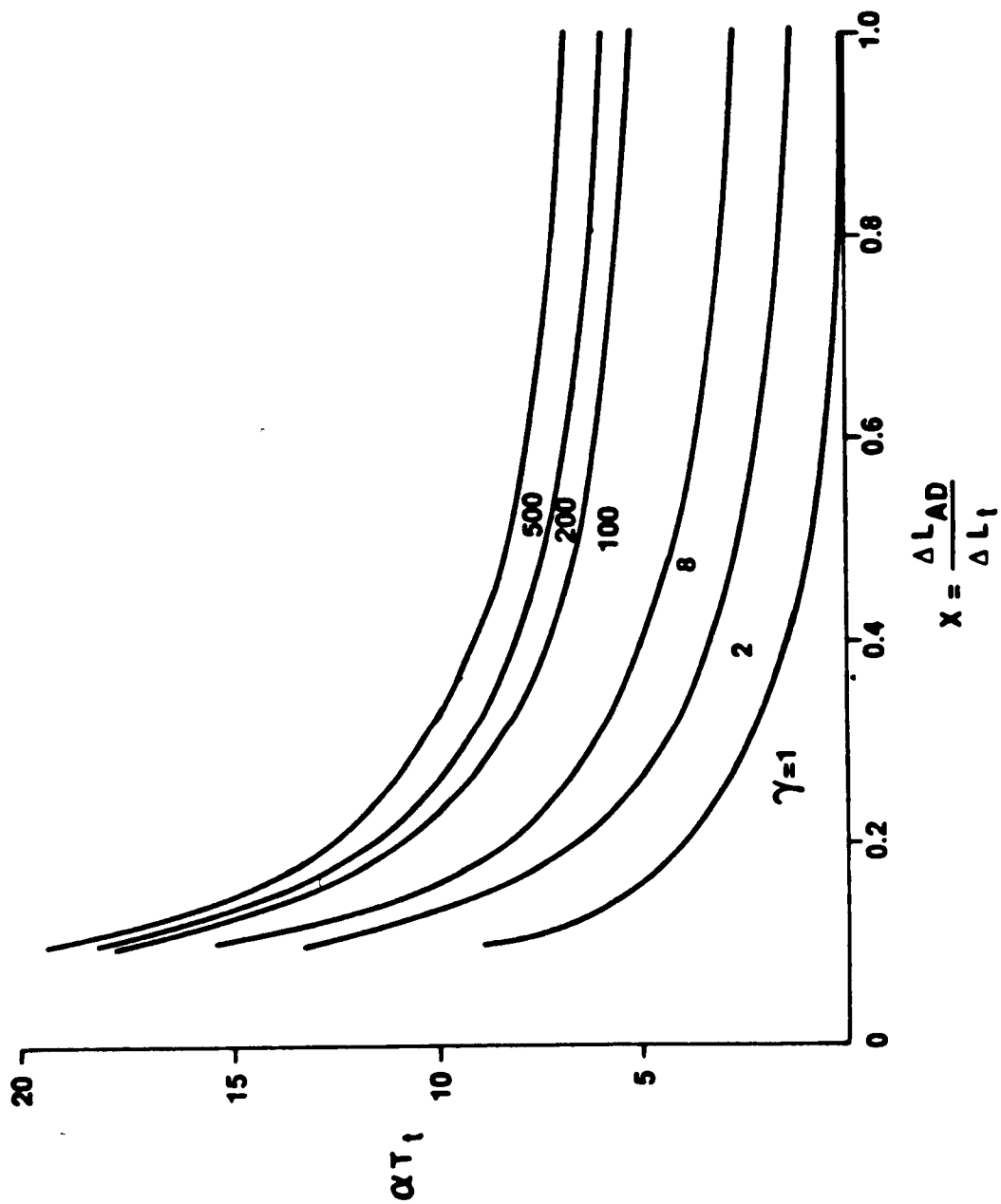


DECELERATION PHASE

DISTANCE

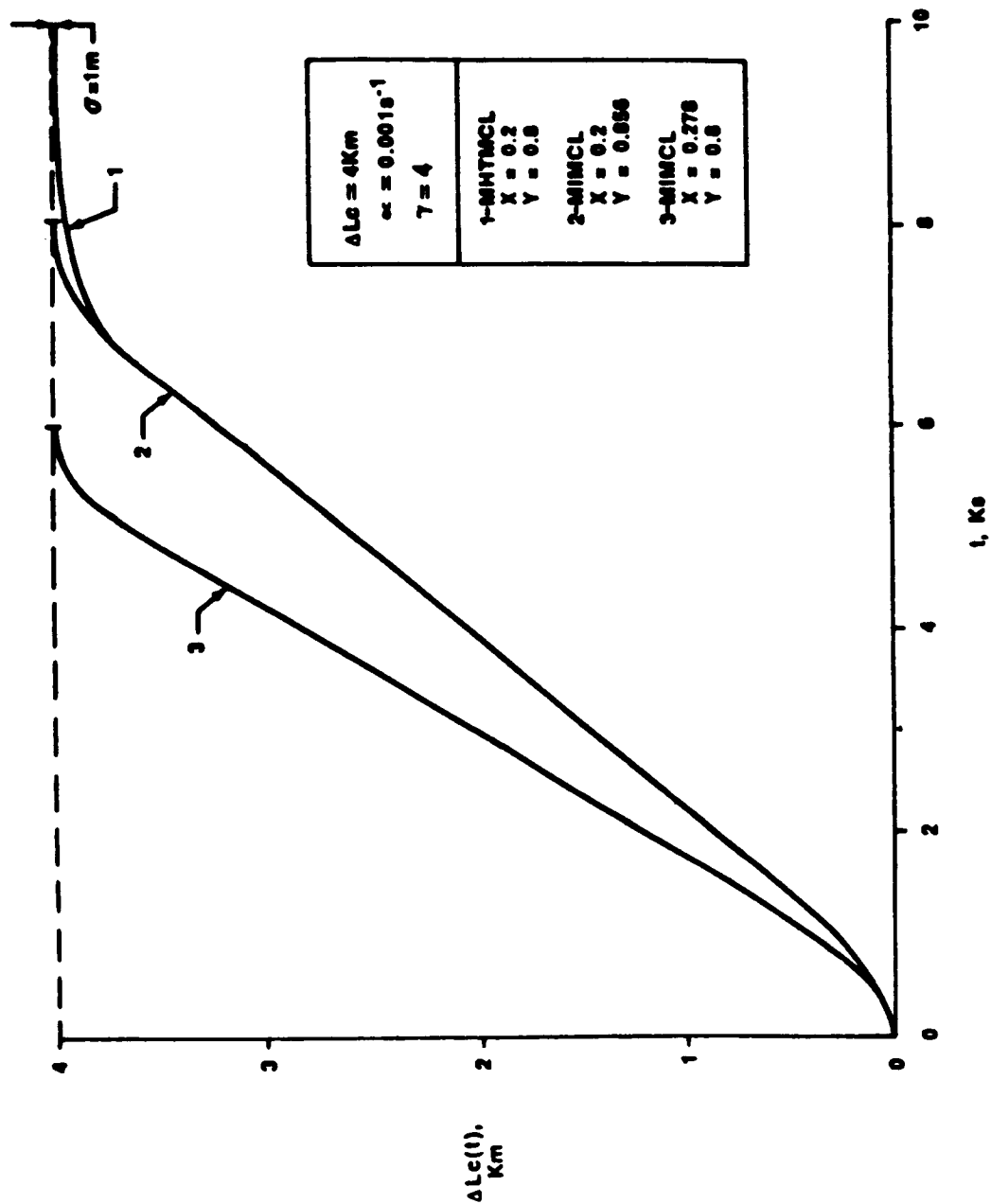
VELOCITY

FIG 3 THREE SUCCESSIVE PHASES OF THE MIRROR IMAGE MOTION CONTROL LAW



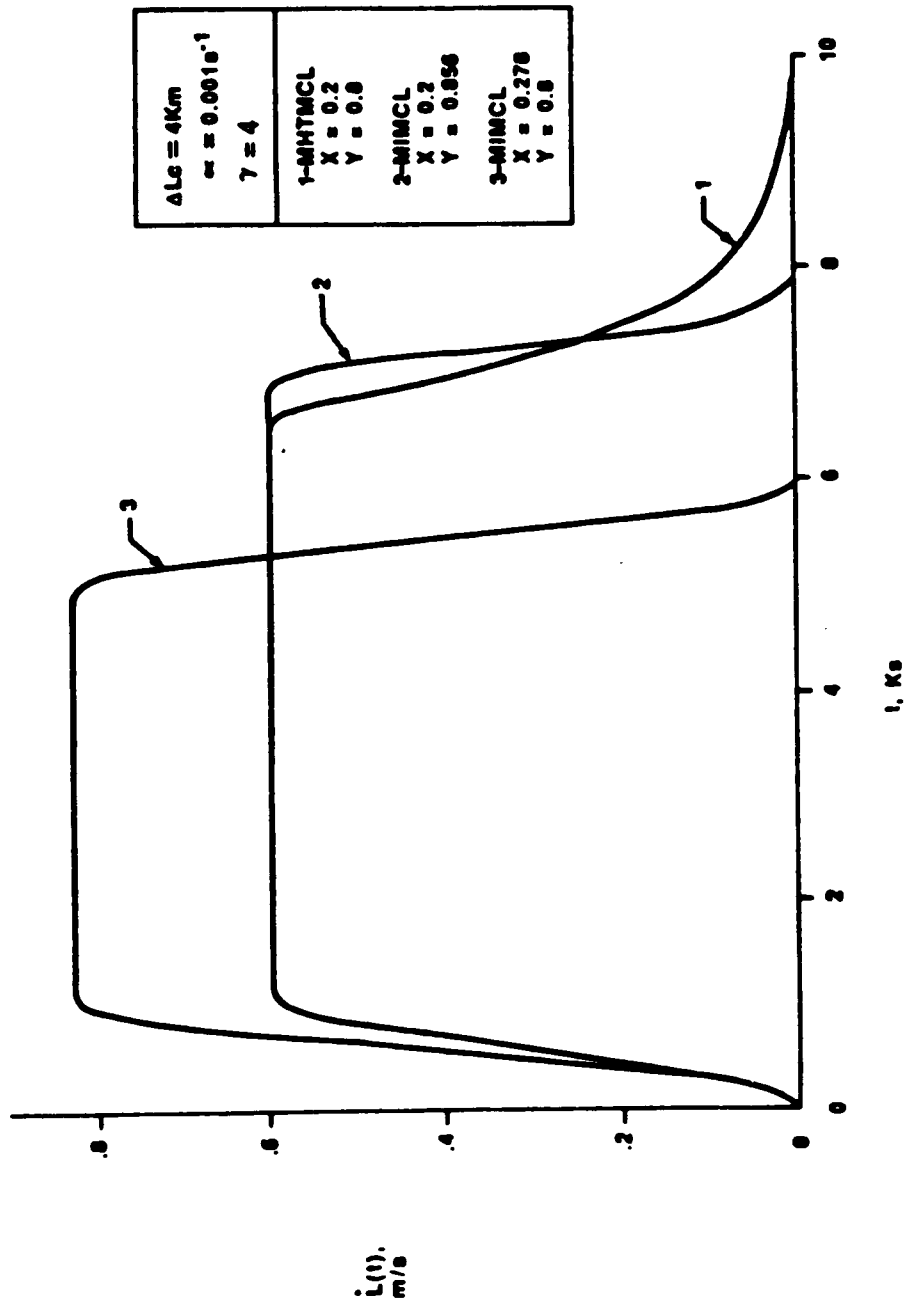
TIME TO TRAVEL TOTAL DISTANCE
MIRROR IMAGE MOTION CONTROL LAW

FIG 4



COMPARISON OF MOTION CONTROL LAWS
DISTANCE TRAVELED VERSUS TIME

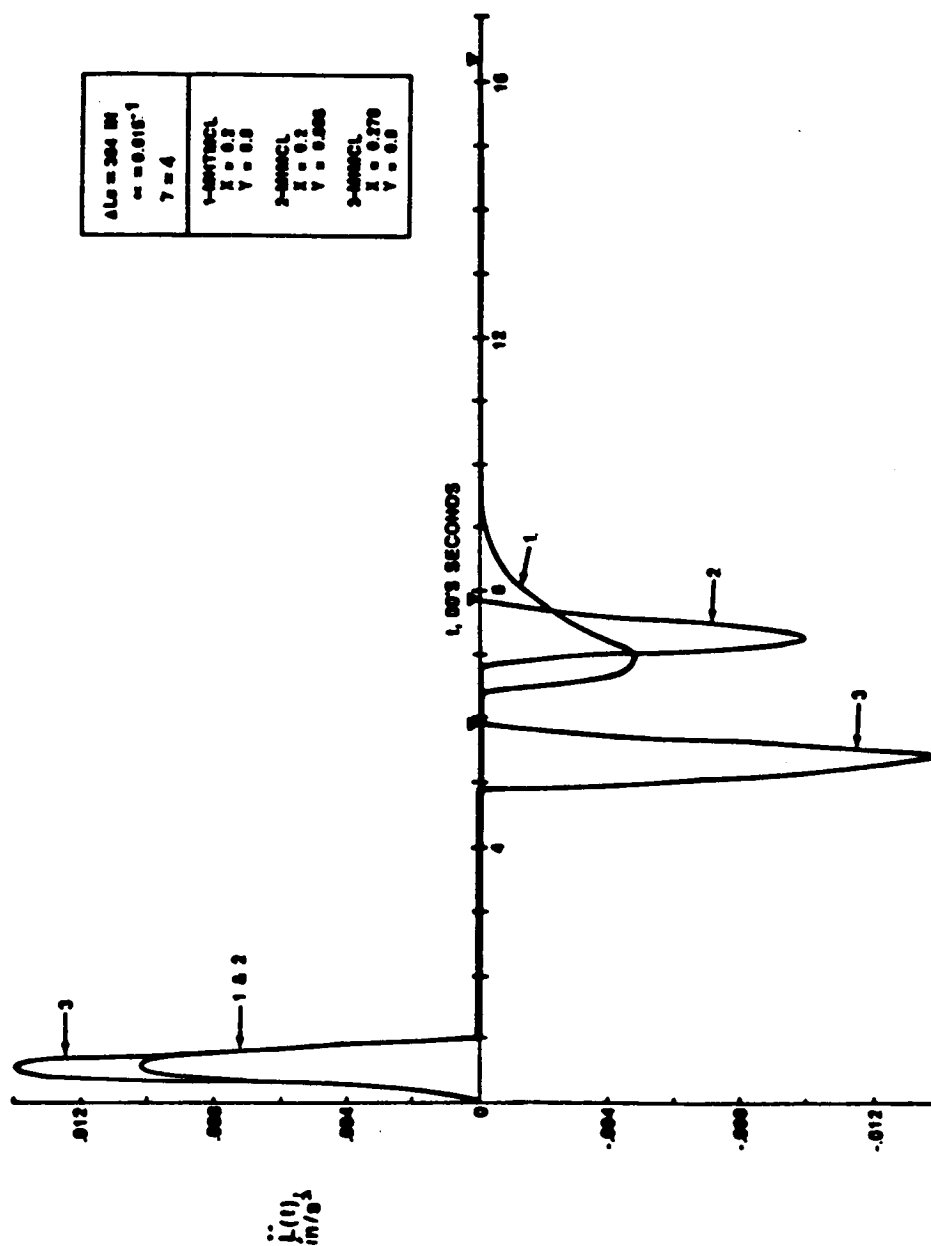
FIG 5



COMPARISON OF MOTION CONTROL LAWS
VELOCITY VERSUS TIME

FIG 6

ORIGINAL PAGE IS
OF POOR QUALITY



ACCELERATION VERSUS TIME
COMPARISON OF MOTION CONTROL LAWS

FIG 7

ORIGINAL PAGE IS
OF POOR QUALITY

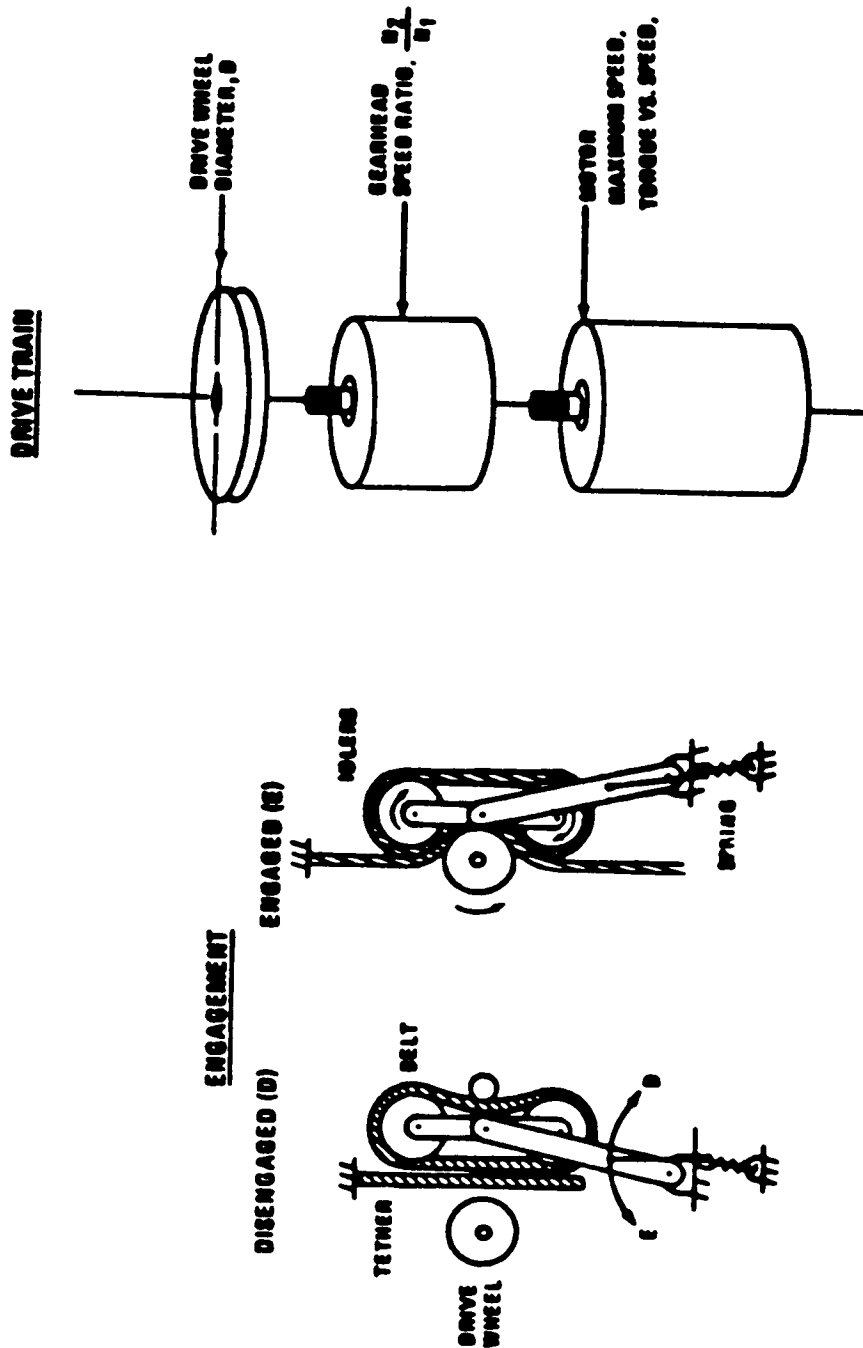


FIG 8 TETHER CRAWLER ENGAGEMENT MECHANISM AND DRIVE TRAIN

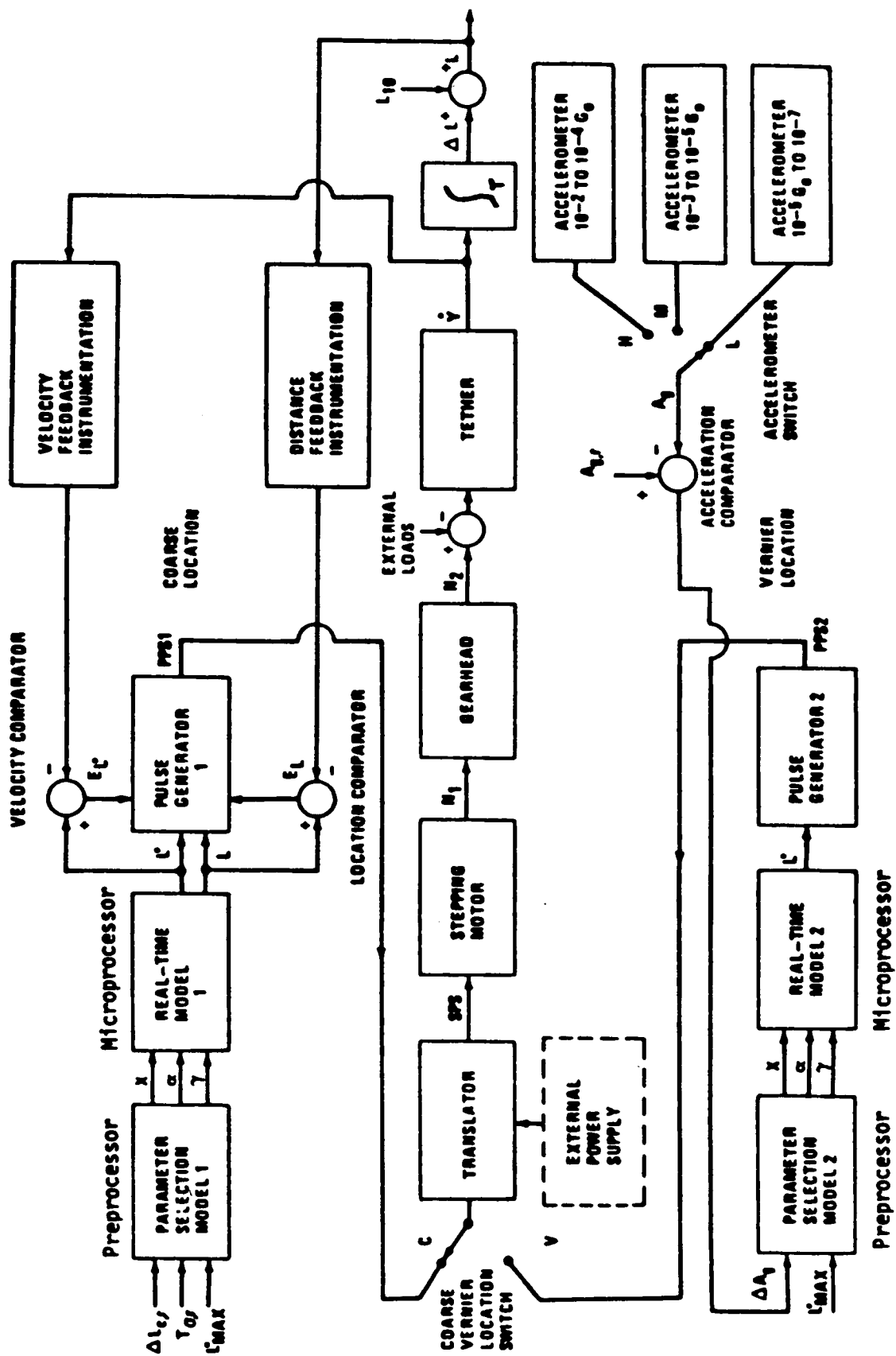
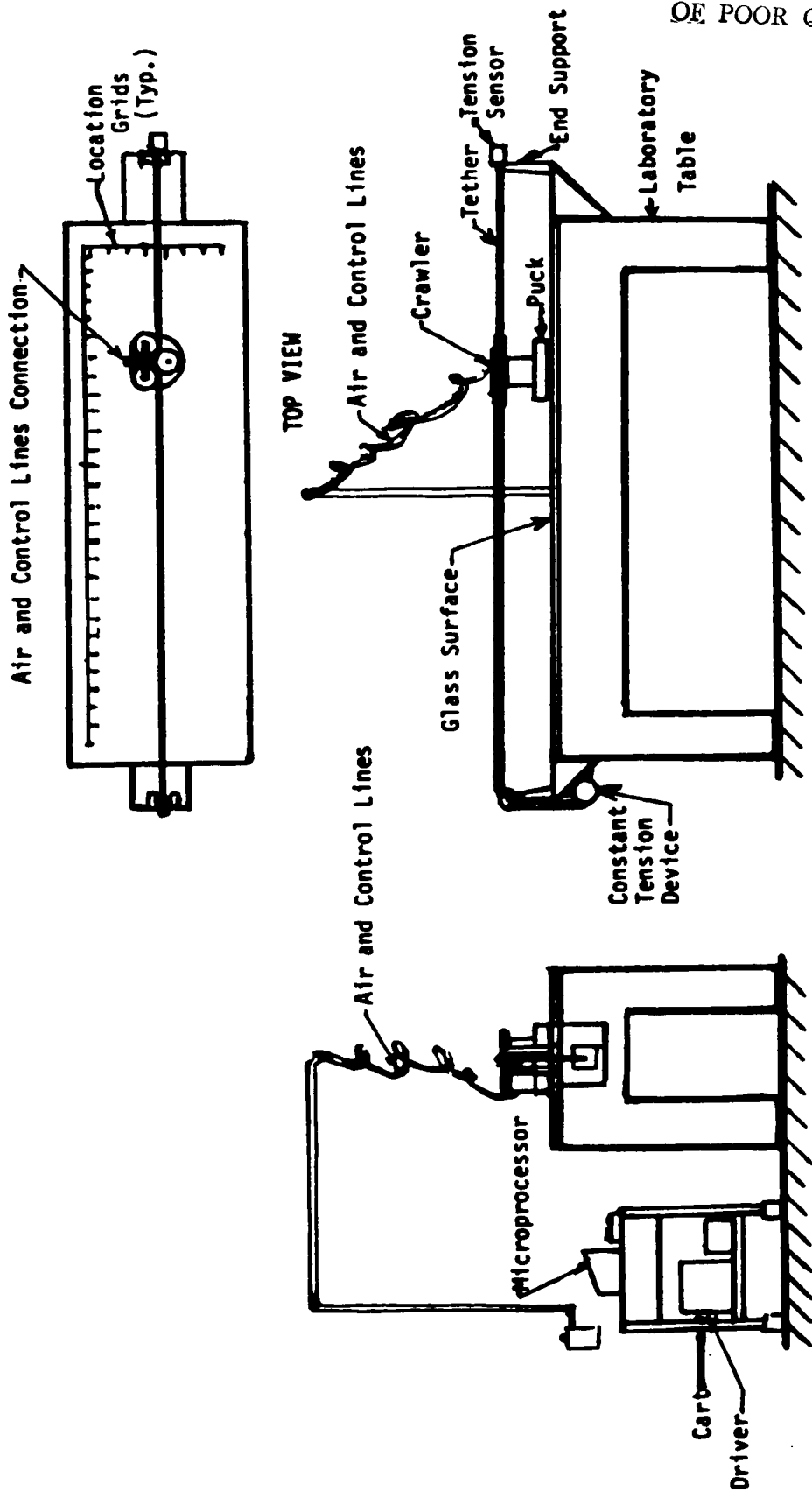


FIGURE 9 DRIVE CONTROL SYSTEM



ORIGINAL PAGE IS
OF POOR QUALITY

SIDE VIEW; Configuration Shown:
Constant Longitudinal Tension and
Free Lateral Position

FIGURE 10 6-FT AIR TABLE

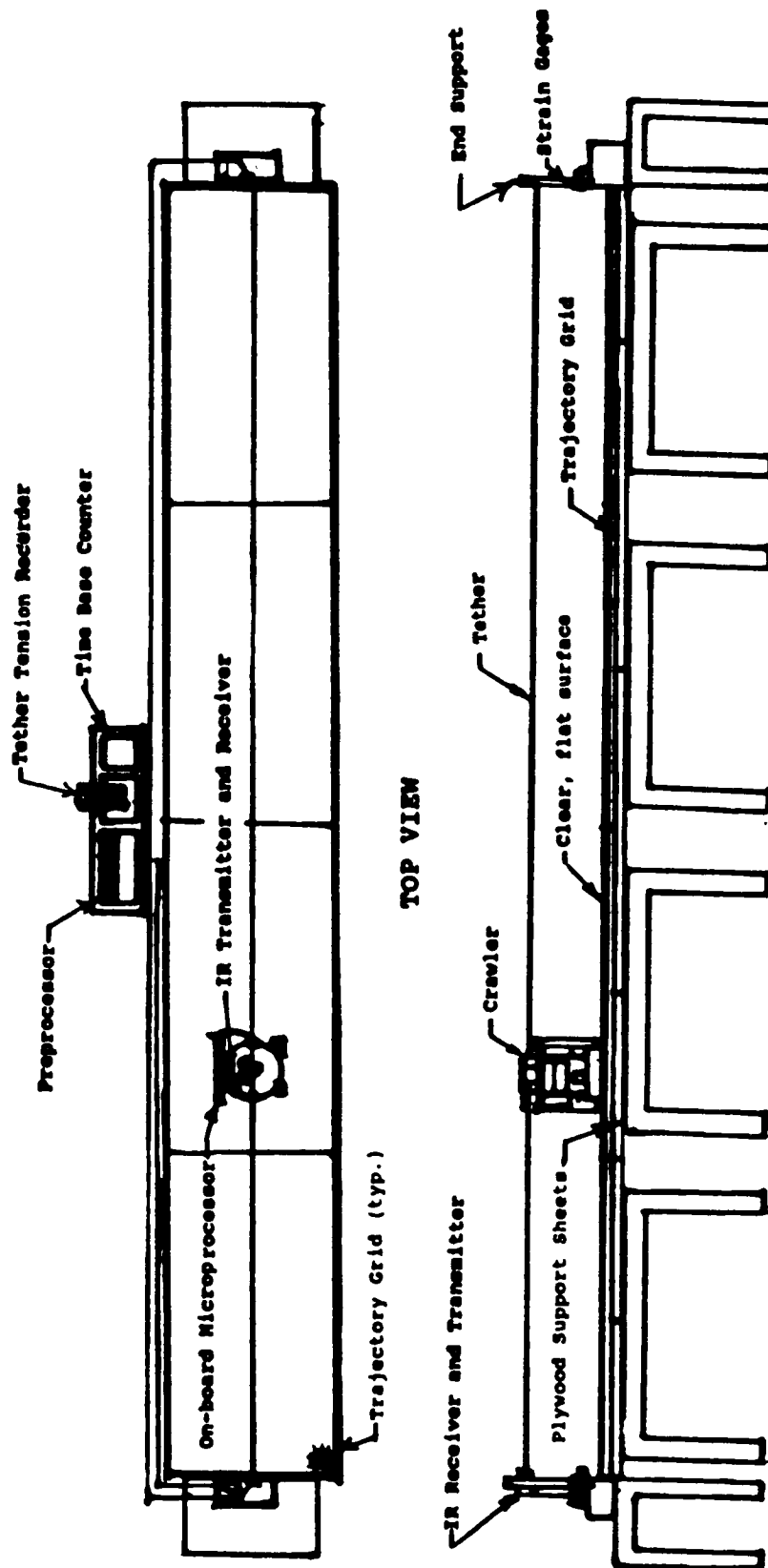


FIGURE 11 32-FOOT AIR TABLE

ORIGINAL PAGE IS
OF POOR QUALITY

ITEMS	SU87	F87	W88	SP88	SU88	F88	W89	SP89	SU89	F89	W90	SP90
DESIGN & OPERATIONS PARAMETERS DEFINITION:												
CRAWLER												
TETHER WEAR VS. GRIP												
LABORATORY TESTS:												
2-D CRAWLER (C) (32-FT)												
(60-FT)												
3-D CRAWLER (C&P)												
DEMONSTRATION FLIGHTS:												
BALLOON (P)												
KC-135 (C)												
ROCKET TO LEO (P)												
SHUTTLE (C & P)												

C - CLOTHESLINE TETHER (FIXED ENDS)
P - PENDANT TETHER (FREE END)

TECS SCHEDULE 1987 - 1990

FIG 12

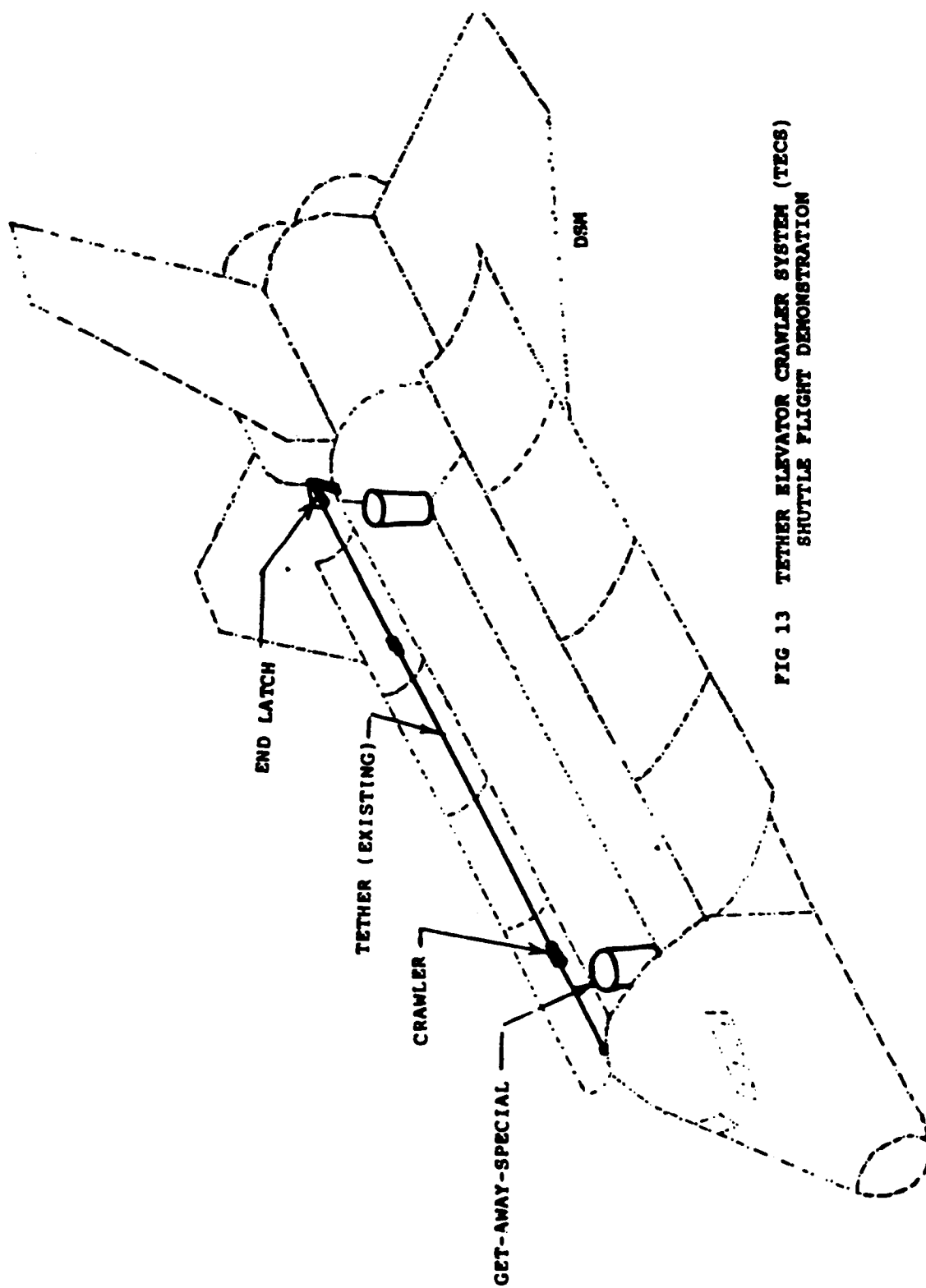


FIG 13 TETHER ELEVATOR CRAWLER SYSTEM (TECS)
SHUTTLE FLIGHT DEMONSTRATION

REFERENCES

1. Rupp, C.L., A Tether Tension Control Law for Tethered Subsatellites Deployed Along the Local Vertical, NASA TMX-94963, Marshall Space Flight Center, September, 1975.
2. Lorenzini, E. C., "A Three-Mass Tethered System for Micro-g/Variable-g Applications", Journal of Guidance, Control and Dynamics, Vol.10, No.3, May-June 1987, pp.242-249.
3. Swenson, Frank R., "Tether Crawler System", Research Projects - 1986, NASA/ASEE Summer Faculty Fellow Program, NASA CR-178966, November, 1986.
4. Swenson, Frank R., First Moves: Tether Elevator Crawler System (TECS), submitted for publication, 1987.
5. Lorenzini, E.C., Analytical Investigation of the Dynamics of Tethered Constellations in Earth Orbit (Phase II), Smithsonian Astrophysical Observatory, Quarterly Report No. 9 for NASA/MSFC under Contract NAS8-36606, July, 1987.